

RESEARCH

Open Access



# Iron oxide polyaniline-coated nanoparticles modulate tumor microenvironment in breast cancer: an in vitro study on the reprogramming of tumor-associated macrophages

Camila Sales Nascimento<sup>1</sup>, Naiara Clemente Tavares<sup>1</sup>, Izabella Cristina Andrade Batista<sup>1</sup>, Mônica Maria Magalhães Caetano<sup>1</sup>, Eneida Santos de Oliveira<sup>2</sup>, Stella Garcia Colombarolli<sup>3</sup>, Anna Carolina Pinheiro Lage<sup>5</sup>, Rodrigo Corrêa-Oliveira<sup>1</sup>, Érica Alessandra Rocha Alves<sup>1</sup>, Celso Pinto de Melo<sup>4</sup> and Carlos Eduardo Calzavara-Silva<sup>1\*</sup>

\*Correspondence:  
carlos.calzavara@fiocruz.br

<sup>1</sup> Grupo de Pesquisa em Imunologia Celular e Molecular, Instituto René Rachou, Fiocruz Minas, Av. Augusto de Lima, 1715, Barro Preto, Belo Horizonte, MG 30190-002, Brazil

<sup>2</sup> Gerência da Rede Ambulatorial Especializada, Secretaria Municipal de Saúde de Belo Horizonte, Prefeitura de Belo Horizonte, 2336 Afonso Pena Avenue, Belo Horizonte 301300-007, Brazil

<sup>3</sup> Istituto di Scienze e Tecnologie Chimiche (SCITEC-CNR), National Research Council of Italy, Roma, Italy

<sup>4</sup> Grupo de Polímeros Não-Convencionais, Departamento de Física, Universidade Federal de Pernambuco, Av. Prof. Moraes Rego, 1235, Cidade Universitária, Recife, PE 50670-901, Brazil

<sup>5</sup> Grupo de Biotecnologia Aplicada ao Estudo de Patógenos, Instituto René Rachou, Fiocruz Minas, Av. Augusto de Lima, 1715 –Barro Preto, Belo Horizonte, MG 30190-002, Brazil

## Abstract

**Background:** Breast cancer is the neoplastic disease with the highest incidence and mortality in the female population worldwide. Treatment remains challenging due to various factors. Therefore, it is of great importance to develop new therapeutic strategies that promote the safe destruction of neoplastic cells without compromising patients' quality of life. Among advances in the treatment of breast cancer, immunotherapy stands out as a promising trend. Recent studies have demonstrated the potential of iron oxide nanoparticles in promoting the reprogramming of M2 macrophages (pro-tumor phenotype) into M1 macrophages (anti-tumor phenotype) within the tumor microenvironment, resulting in potent antitumor effects. In this study, the effect of polyaniline-coated iron oxide nanoparticles (Pani/γ-Fe<sub>2</sub>O<sub>3</sub>) on macrophage polarization and breast cancer cell death was investigated.

**Methods:** The non-cytotoxic concentration of nanoparticles was determined using the MTT assay. For in vitro co-culture experiments, breast cancer cell lines MCF -7 and MDA-MB -231 and macrophages THP-1 were co-cultured in a Transwell system and then the effects of Pani/γ-Fe<sub>2</sub>O<sub>3</sub> on cell viability, gene expression, cytokine profile, and oxidative stress markers were investigated.

**Results:** The results showed that Pani/γ-Fe<sub>2</sub>O<sub>3</sub> nanoparticles induced M2-to-M1 macrophage polarization in both cell lines through different pathways. In MCF -7 and THP-1 macrophage co-culture, the study showed a decrease in cytokine levels IL -1β, upregulation of M1-associated genes (*IL-12*, *TNF-α*) in macrophages, resulting in increased MCF -7 cell death by apoptosis (caspase 3/7<sup>+</sup>). In MDA-MB -231 co-cultures, increases in cytokines IL -6, IL -1β, and oxidative stress markers were observed, as well as upregulation of the inducible nitric oxide synthase (*iNOS*) gene in macrophages, leading to tumor cell death via apoptosis-independent pathways (Sytox<sup>+</sup>).



**Conclusions:** These findings highlight the potential of Pani/ $\gamma$ -Fe<sub>2</sub>O<sub>3</sub> as a promising therapeutic approach in the context of breast cancer treatment by effectively reprogramming M2 macrophages into an anti-tumor M1 phenotype, Pani/ $\gamma$ -Fe<sub>2</sub>O<sub>3</sub> nanoparticles demonstrated the ability to elicit antitumor effects in both MCF-7 and MDA-MB-231 breast cancer cell lines.

**Keywords:** Breast cancer, Tumor-associated macrophages (TAMs), Macrophages, Polarization, Iron oxide nanoparticles, Tumor microenvironment, Immunotherapy, Nanotechnology

## Introduction

Breast cancer has overtaken lung cancer as the most prevalent form of cancer worldwide. It accounts for about 24.5% of all cancer cases worldwide and is responsible for about one in eight cancer diagnoses, with a total of 2.3 million new cases (Sung et al. 2021; Arnold et al. 2022). In women, breast cancer remains a major public health problem, accounting for one in four cancers and one in six cancer-related deaths. In most countries, breast cancer is the most common cancer (159 out of 185 countries) and the main cause of cancer-related deaths in 110 countries (Sung et al. 2021). Therefore, developing new initiatives and strategies to prevent and treat breast cancer is critical to reducing breast cancer mortality rates, promoting breast health, and ensuring equitable access to quality care.

Treatment for breast cancer often consists of a combination of surgical removal, radiation therapy, hormone therapy, and chemotherapy. These treatments can reduce breast cancer recurrence and mortality but may increase the risk of death from other diseases (Harbeck and Gnant 2017). Evidence on the benefits and risks of these treatments is not static but is continually accumulating and scattered in the literature (Kerr et al. 2022). Despite advances in early detection and understanding of the molecular basis of breast cancer biology, approximately 30% of breast cancer patients experience disease recurrence (Colleoni et al. 2016).

To address these challenges, innovative approaches to breast cancer treatment are currently being explored, including immunotherapies that stimulate the immune system to attack cancer cells and combination therapies that integrate different treatment modalities. In this context, the tumor microenvironment is an important target for the development of new therapies.

The tumor microenvironment consists not only of the tumor mass but also of a variety of leukocytes, fibroblasts, extracellular matrix, and various bioactive molecules derived from both tumor and non-tumor cells that play a critical role in regulating tumor growth and invasiveness (Huang et al. 2017). Among these important cells, tumor-associated macrophages (TAMs) have attracted great interest as a therapeutic target in recent years due to their high contribution to the cellular component of the tumor microenvironment.

The historical classification of macrophage activation states into a simplified binary categorization of M1 and M2 has provided a framework for understanding their distinct roles in the tumor microenvironment (Murray et al. 2014). M1 macrophages, characterized by their pro-inflammatory phenotype, play a critical role in promoting the Th1 immune response by producing key cytokines such as TNF- $\alpha$ , IL-1 $\beta$ , and IL

-12 as well as generating reactive oxygen species (ROS) and reactive nitrogen species (RNS) (Weagel et al. 2015). These effector molecules exert potent cytotoxic effects, facilitate tumor cell destruction, and contribute to antitumor immunity (Mantovani et al. 2017). M2 macrophages, on the other hand, also known as alternatively activated macrophages, exhibit an anti-inflammatory phenotype and are involved in immune regulation and tissue remodeling (Biswas and Mantovani 2012). They are known to promote the Th2 immune response and secrete significant amounts of immunomodulatory molecules such as IL -10, TGF- $\beta$ , and various chemokines (Mantovani et al. 2017, 2004). M2 macrophages possess weak antigen-presenting abilities, attenuate Th1 responses, and contribute to the attenuation of inflammation. In addition, they are actively involved in processes that promote tumor progression, such as angiogenesis and tissue remodeling (Biswas and Mantovani 2010).

In recent years, the field of immunometabolism has witnessed a significant surge of interest, with numerous studies focusing on the reprogramming of macrophages through cellular metabolism modification. Various approaches have been proposed to modulate TAMs, aiming to shift their phenotype towards an M1-like state. Among the metabolic characteristics crucial for differentiating macrophage phenotypes, iron metabolism has been recognized as a significant factor, as macrophage polarization closely correlates with intracellular iron levels (Biswas and Mantovani 2012; Corna et al. 2010). M1 macrophages exhibit high levels of ferritin and low levels of ferroportin, CD163, and Heme Oxygenase-1, favoring an intracellular iron sequestration and storage phenotype (Cronin et al. 2019; Jung et al. 2019). Conversely, M2 macrophages demonstrate an iron export phenotype characterized by increased expression of CD163 and Heme Oxygenase-1, as well as high expression of ferroportin and reduced expression of ferritin (Recalcati and Cairo 2021).

Studies have revealed that iron oxide nanoparticles (IONPs) can influence TAMs polarization, reprogramming these cells to relinquish their tumor-promoting function and adopt tumor-suppressive properties. Previous *in vitro* studies by Laskar et al. (2013) demonstrated that IONPs induce a phenotypic shift in M2 macrophages towards an M1 macrophage subtype (Laskar et al. 2013). This finding has been corroborated by subsequent studies (Zanganeh et al. 2016; Costa da Silva et al. 1479; Zhang et al. 2020; Zhou et al. 2020). Consequently, there is immense potential in developing novel, cost-effective iron-based nanoparticles that effectively polarize macrophages toward an M1 phenotype. Such advancements would not only complement existing breast cancer treatment strategies but also expand treatment accessibility for patients afflicted by this disease.

A previous study conducted by our research group demonstrated that iron oxide polyaniline-coated nanoparticles (Pani/ $\gamma$ -Fe<sub>2</sub>O<sub>3</sub> NPs) were capable of modulating macrophage polarization to the M1 phenotype in 3D multicellular models of breast cancer (Nascimento et al. 2023). Building upon these findings, the present study aimed to further investigate the effect of Pani/ $\gamma$ -Fe<sub>2</sub>O<sub>3</sub> NPs on the reprogramming of TAMs in an *in vitro* setting, as well as to evaluate its impact on different human breast tumor cell lines. Considering that iron exposure impact on macrophage polarization states, Pani/ $\gamma$ -Fe<sub>2</sub>O<sub>3</sub> NPs hold promise in regulating macrophage polarization, offering fresh insights into the role of intracellular iron regulation in macrophage function. This research sets

the stage for the development of cutting-edge anticancer technologies based on IONPs (Additional file 1).

## Results

### Biocompatibility

To ensure the biocompatibility of Pani/ $\gamma$ -Fe<sub>2</sub>O<sub>3</sub> NPs, their cytotoxicity to tumor cells and macrophages was evaluated using the MTT assay. After analyzing the data obtained from tumor cells, it was found that the maximum noncytotoxic concentration for MCF-7 and MDA-MB-231 was 3 mg/mL and 1.5 mg/mL, respectively (Fig. 1a and b).

Regarding THP-1 macrophages, the results showed that the maximum noncytotoxic concentration of Pani/ $\gamma$ -Fe<sub>2</sub>O<sub>3</sub> NPs was 0.06 mg/mL (Fig. 1c). Given the lower tolerance of macrophages to exposure to Pani/ $\gamma$ -Fe<sub>2</sub>O<sub>3</sub> NPs compared with the tumor cells used in this study, the maximum noncytotoxic concentrations obtained for macrophages were selected for in vitro transwell assays. The internalization of Pani/ $\gamma$ -Fe<sub>2</sub>O<sub>3</sub> nanoparticles by THP-1 macrophages was validated through of brightfield microscopy images and transmission electron microscopy micrographs (Additional file 1: Fig. S2a and S2b).

### Effect of Pani/ $\gamma$ -Fe<sub>2</sub>O<sub>3</sub> NPs on tumor cells viability

To evaluate tumor cell viability after exposure of NPs to macrophages, MCF-7 and MDA-MB-231 were cultured with THP-1 macrophages using a 0.4  $\mu$ m transwell

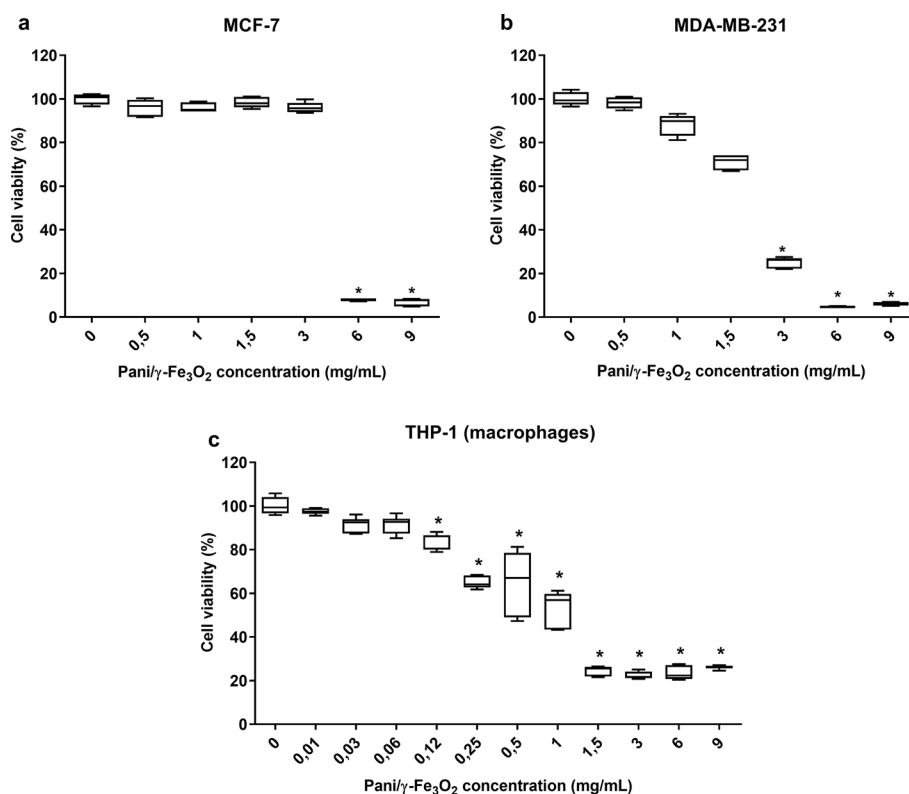


**Fig. 1** In **a** MCF-7 cell viability (%). In **b** MDA-MB-231 cell viability (%). In **c** THP-1 macrophages cell viability (%). The data are presented as median, quartiles, and extremes and represent three independent experiments. Statistical analysis was performed using Kruskal–Wallis followed by Dunn’s test. \*p < 0.05

membrane system. A culture medium with or without 0.06 mg/mL Pani/ $\gamma$ -Fe<sub>2</sub>O<sub>3</sub> NPs was added to the upper chamber containing the macrophages. Co-culturing was performed for 24 and 48 h. After the incubation period, the frequency of nonviable (Sytox<sup>+</sup>) and apoptotic (caspase 3/7<sup>+</sup>) tumor cells was evaluated.

The results show that after 24 h of co-cultivation with macrophages, there were no significant differences between the expression levels of MCF -7 caspase 3/7 (Fig. 2a). However, after 48 h of co-cultivation, a higher percentage of apoptotic MCF -7 cells was observed in cultures containing macrophages co-cultured with tumor cells. Remarkably, during the same incubation period, an even higher percentage of apoptotic MCF -7 cells was observed in cultures containing macrophages exposed to Pani/ $\gamma$ -Fe<sub>2</sub>O<sub>3</sub> NPs, indicating that the presence of nanoparticles increases the pro-apoptotic capacity of macrophages (p = 0.0286, paired t-test; Fig. 2a). The MCF -7 cells were also labeled with Sytox (48 h) to assess cell death via other pathways. Interestingly, we found that incubation with macrophages and/or exposure to Pani/ $\gamma$ -Fe<sub>2</sub>O<sub>3</sub> NPs did not significantly affect the percentage of non-viable MCF -7 cells in the co-cultures.

For co-culture with the MDA-MB-231 cell line, no significant differences were observed between the percentages of cells expressing active caspase 3/7 at either incubation time (Fig. 2b). Regarding labeling of nonviable cells, it was observed that co-culture with macrophages and exposure to Pani/ $\gamma$ -Fe<sub>2</sub>O<sub>3</sub> NPs did not significantly alter the percentage of cell death in tumor cells at 24 h. However, after 48 h, exposure to Pani/ $\gamma$ -Fe<sub>2</sub>O<sub>3</sub> NPs was able to increase the percentage of non-viable tumor cells (Sytox<sup>+</sup>) in the co-culture system (p = 0.0161, paired t-test, Fig. 2b).

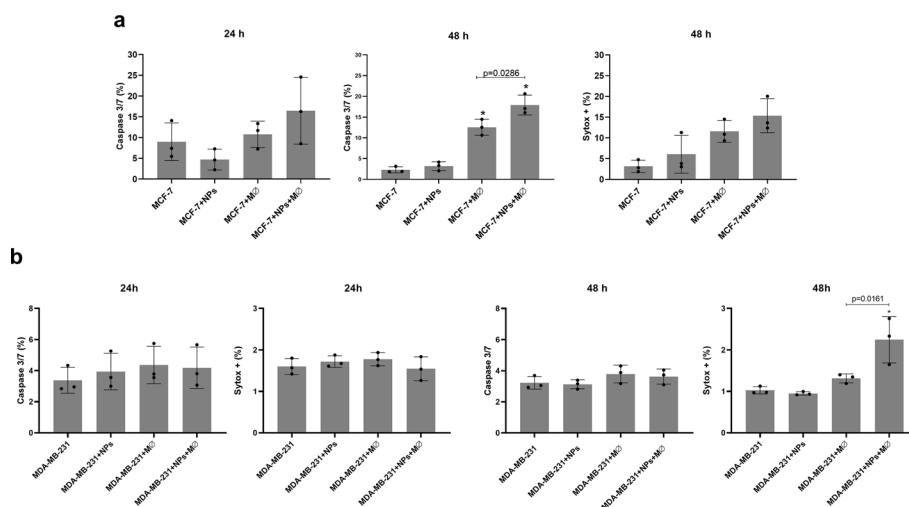


**Fig. 2** In **a** Frequency of MCF-7 cells expressing active caspase 3/7 after 24 h of co-culture and labeled with Sytox after 24 h and 48 h of co-culture. In **b** Frequency of MDA-MB-231 cells expressing active caspase 3/7 and labeled with Sytox after 24 h and 48 h of co-culture. The data are presented as mean  $\pm$  standard deviation and represent three independent experiments. Statistical analysis was performed using paired t-test. (\*) p < 0.05 compared to the unstimulated tumor cell. (Bar) p < 0.05 between co-cultures of tumor cells and macrophages exposed and unexposed to NPs, p-value indicated in the graph. NPs = Pani/ $\gamma$ -Fe<sub>2</sub>O<sub>3</sub>; MØ = macrophages

### Effect of Pani/ $\gamma$ -Fe<sub>2</sub>O<sub>3</sub> NPs on cytokine profile

The tumor microenvironment promotes the secretion of various cytokines that may inhibit tumor development, but they may also contribute to chronic inflammation that promotes growth. Therefore, we investigated the effect of NPs on the production of anti-/pro-inflammatory cytokines in co-cultures between tumor cells and macrophages using a cytometric bead array.

In cultures containing only MCF-7 cells, only IL-6 cytokine was detected after 48 h of incubation (Fig. 3b). In cultures containing only macrophages, the cytokines IL-1 $\beta$ , IL-8, IL-6, and TNF- $\alpha$  were detected at both time points examined, with higher levels of IL-8 and TNF- $\alpha$  than IL-1 $\beta$  and IL-6 (Fig. 3).

Co-incubation of macrophages and MCF-7 cells resulted in higher levels of IL-1 $\beta$ , IL-6, and IL-8 at both incubation times compared with cultures containing only macrophages or MCF-7 cells (Fig. 3), suggesting that co-culture between cells modulates production of these cytokines. The addition of Pani/ $\gamma$ -Fe<sub>2</sub>O<sub>3</sub> NPs significantly decreased IL-1 $\beta$  levels in the cell-free co-culture medium after 24 h ( $p = 0.0173$ , paired t-test; Fig. 3a) compared to co-culture without NPs.

For co-culture between MDA-MB-231 cells and THP-1 macrophages, it was observed that the cytokine IL-12p70 was not produced under the conditions and controls studied

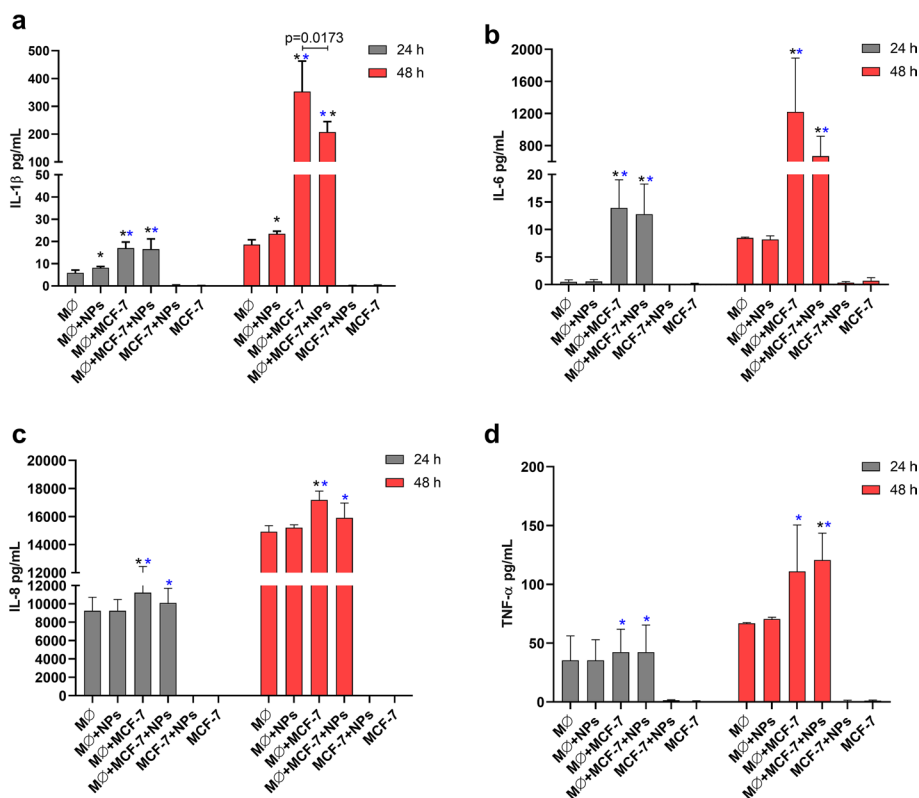


**Fig. 3** In **a** IL-1 $\beta$  (pg/mL). In **b** IL-6 (pg/mL). In **c** IL-8 (pg/mL). In **d** TNF- $\alpha$  (pg/mL). The data are presented as mean  $\pm$  standard deviation and represent three independent experiments. Statistical analysis was performed using paired t-test. (\*)  $p < 0.05$  compared to the unstimulated macrophage. (\*\*)  $p < 0.05$  compared to the unstimulated tumor cells. (Bar)  $p < 0.05$  between co-cultures containing tumor cells and macrophages exposed and unexposed to NPs, p-value indicated in the graph. NPs = Pani/ $\gamma$ -Fe<sub>2</sub>O<sub>3</sub>; MØ = macrophages

(Fig. 4). Cell-free culture medium from cultures containing only MDA-MB-231 cells showed measurable levels of IL-1 $\beta$ , IL-8, IL-6, TNF- $\alpha$ , and IL-10 (Fig. 4). The medium from cultures containing only macrophages showed detectable levels of IL-1 $\beta$ , IL-8, TNF- $\alpha$ , and IL-10 at both study time points, with levels of IL-8 and TNF- $\alpha$  higher than those of IL-1 $\beta$  and IL-10.

When macrophages and MDA-MB-231 cells were incubated together, it was observed that the cell-free culture medium had higher levels of IL-6 at both incubation times

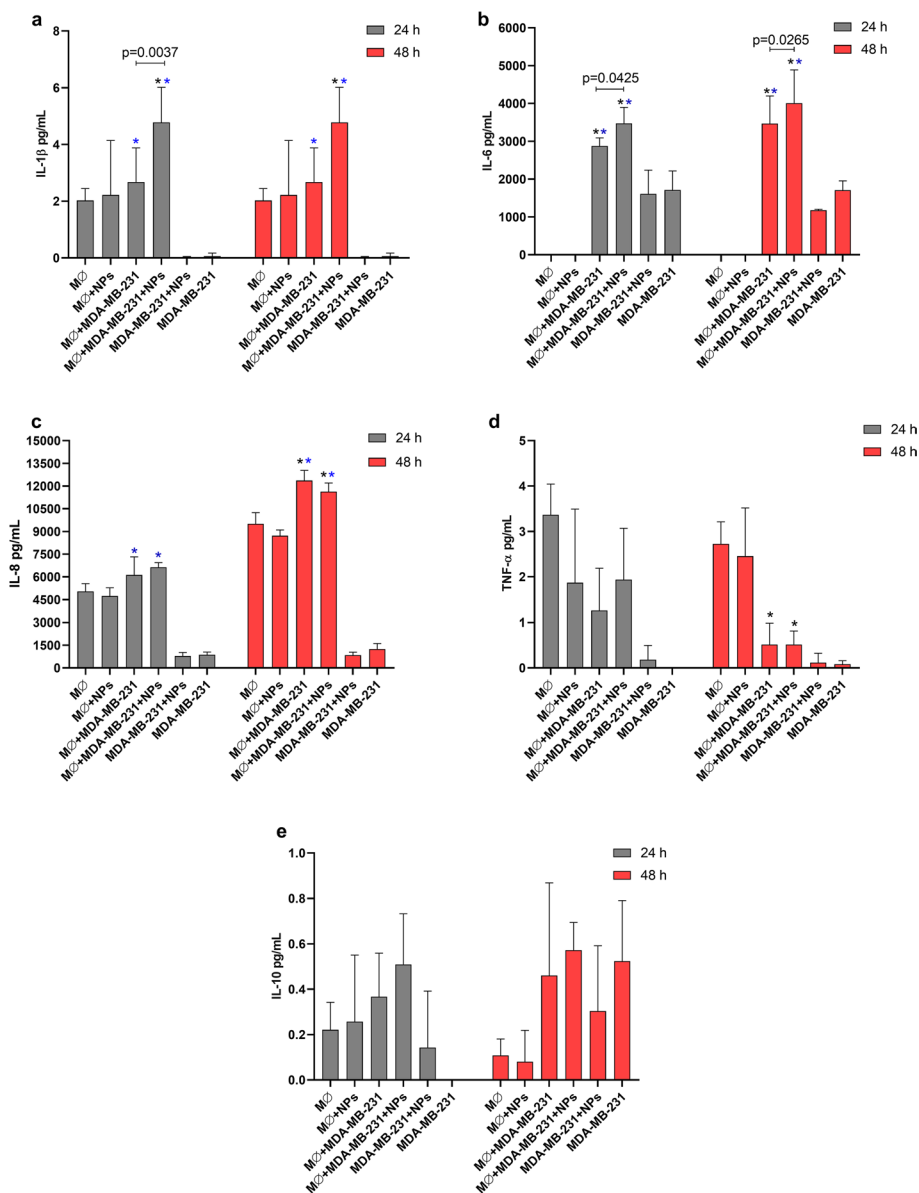


**Fig. 4** In **a** IL-1 $\beta$  (pg/mL). In **b** IL-6 (pg/mL). In **c** IL-8 (pg/mL). In **d** TNF- $\alpha$  (pg/mL). In **e** IL-10 (pg/mL). The data are presented as mean  $\pm$  standard deviation and represent three independent experiments. Statistical analysis was performed using paired t-test. (\*)  $p < 0.05$  compared to the unstimulated macrophage. (\*)  $p < 0.05$  compared to the unstimulated tumor cells. (Bar)  $p < 0.05$  between co-cultures containing tumor cells and macrophages exposed and unexposed to NPs,  $p$ -value indicated in the graph. NPs = Pani/ $\gamma$ -Fe $_2$ O $_3$ ; M $\phi$  = macrophages

(Fig. 4b) and IL-8 after 48 h (Fig. 4c) than cultures containing only macrophages or MDA-MB-231 cells. On the other hand, the cell-free medium from co-cultures had lower TNF- $\alpha$  levels compared with cultures containing only macrophages (Fig. 4d). These results suggest that co-culture between these cells may significantly modulate the production of the cytokines IL-6, IL-8, and TNF- $\alpha$ .

When co-cultures were compared in the absence and presence of Pani/ $\gamma$ -Fe<sub>2</sub>O<sub>3</sub> NPs, it was found that the levels of IL-8, TNF- $\alpha$ , and IL-10 remained unchanged at both incubation times evaluated. However, the addition of NPs caused a significant increase in the IL-1 $\beta$  concentration in the cell-free co-culture medium after 24 h ( $p = 0.0037$ , paired t-test, Fig. 4a) and of IL-6 at both incubation times ( $p < 0.05$ , paired t-test; Fig. 4b), indicating that the NPs affect the production of these cytokines in this co-culture system.

The results suggest that tumor cells have the remarkable ability to modulate the tumor microenvironment and influence cytokine production by macrophages through various mechanisms. Such modulation can significantly affect the response to exposure to NPs.

#### Effect of Pani/ $\gamma$ -Fe<sub>2</sub>O<sub>3</sub> NPs on oxidative stress markers

It is well known that increased oxidative stress in the tumor microenvironment can lead to increased tumor cell death via several pathways. The co-culture assays between MCF-7 cells and macrophages showed that the oxidative stress markers assessed (malondialdehyde, carbonylated proteins, and hydrogen peroxide) were detected in all culture conditions analyzed (Fig. 5a–c). In particular, the cell-free co-culture medium exposed to NPs had higher hydrogen peroxide levels than the cultures containing only macrophages (Fig. 5a).

In tests with the cell line MDA-MB-231, indicators of oxidative stress were also detected under all conditions studied, but few differences were observed (Fig. 5d–f). It was demonstrated that co-culture of the cell line MDA-MB-231 with THP-1 macrophages exposed to Pani/ $\gamma$ -Fe<sub>2</sub>O<sub>3</sub> NPs for 24 h resulted in increased levels of protein carbonylation in the co-culture medium compared with cultures containing macrophages alone ( $p < 0.05$ , paired t-test; Fig. 5f). In addition, it was observed that the medium from co-cultured tumor cells and macrophages exposed to NPs had significantly higher hydrogen peroxide levels than the medium from cell controls without stimuli ( $p < 0.05$ , paired t-test; Fig. 5d). After 48 h, higher levels of malondialdehyde ( $p = 0.0422$ , paired t-test; Fig. 5d), protein carbonylation ( $p = 0.0114$ , paired t-test; Fig. 5e), and hydrogen peroxide ( $p = 0.0248$ , paired t-test; Fig. 5f) were found in the medium of co-cultures exposed to NPs.

Overall, the results demonstrated that exposure to Pani/ $\gamma$ -Fe<sub>2</sub>O<sub>3</sub> NPs had minimal effects on oxidative stress indicators in co-cultures with MCF-7 cells. However, in co-cultures containing MDA-MB-231 cells, there was a remarkable increase in indicators of lipid peroxidation, malondialdehyde, and protein carbonylation.

#### Effect of Pani/ $\gamma$ -Fe<sub>2</sub>O<sub>3</sub> NPs on the macrophage gene expression

Because of the close relationship between iron metabolism and macrophage phenotype, IONPs can alter the gene expression of M1 and M2 macrophage markers. Therefore, the effect of Pani/ $\gamma$ -Fe<sub>2</sub>O<sub>3</sub> NPs on gene expression of anti-/pro-inflammatory cytokines, *arginase-1* (*ARG-1*), *iNOS*, and macrophage surface receptors associated



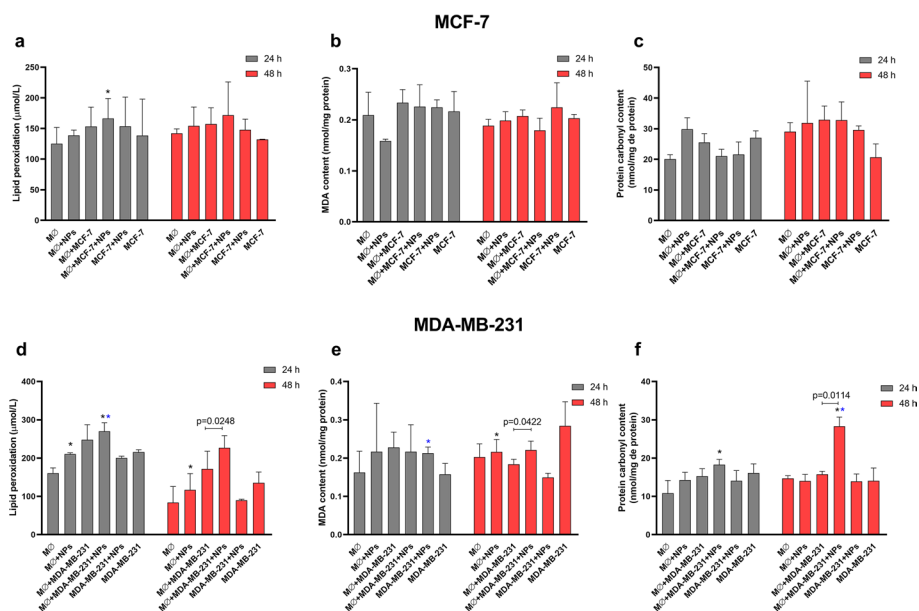


**Fig. 5** In **a** Levels of MDA content (nmol/mg protein) in cell-free co-culture medium of MCF-7 and macrophages; In **b** Levels of protein carbonyl content (nmol/mg protein) in cell-free co-culture medium of MCF-7 and macrophages. In **c** Levels of lipid peroxidation ( $\mu\text{mol/L}$ ) in cell-free co-culture medium of MCF-7 and macrophages. In **d** Levels of MDA content (nmol/mg protein) in cell-free co-culture medium of MDA-MB-231 and macrophages; In **e** Levels of protein carbonyl content (nmol/mg protein) in cell-free co-culture medium of MDA-MB-231 and macrophages; In **f** Levels of lipid peroxidation ( $\mu\text{mol/L}$ ) in cell-free co-culture medium of MDA-MB-231 and macrophages. Data are presented as mean  $\pm$  standard deviation and are representative of three independent experiments. Statistical analysis was performed using paired t-test. (\*)  $p < 0.05$  compared to the unstimulated macrophage. (\*)  $p < 0.05$  compared to the unstimulated tumor cells. (Bar)  $p < 0.05$  between co-cultures containing tumor cells and exposed and non-exposed macrophages to NPs, p-value indicated in the graph. NPs = Pani/ $\gamma\text{-Fe}_2\text{O}_3$ ; M0 = macrophages

with M1 and M2 phenotypes was investigated by qPCR. It was found that *CD86*, *CD80*, and *ARG -1* genes were not expressed at either incubation time (Fig. 6a). THP-1 macrophages showed little change in their gene expression of M1 and M2 markers when co-incubated with MCF-7 cells (Fig. 6a). After 48 h, the expression of *IL-10* was higher in macrophages from co-cultures than in macrophages incubated with the culture medium alone ( $p < 0.05$ , paired t-test). In addition, macrophages co-cultured with MCF-7 cells and exposed to NPs showed increased expression of the *IL-12* gene at 24 h ( $p = 0.0078$ , paired t-test) and the *TNF- $\alpha$*  gene at 48 h ( $p = 0.0453$ , paired t-test).

When co-cultured between MDA-MB-231 cells and THP-1 macrophages, it was observed that macrophages co-cultured with tumor cells and exposed to NPs had increased *iNOS* expression compared to macrophages co-cultured with MDA-MB-231 cells in the absence of NPs ( $p = 0.0200$ , paired t-test) (Fig. 6b).

These results suggest that Pani/ $\gamma\text{-Fe}_2\text{O}_3$  NPs can modulate macrophage polarization in the presence of tumor cells, which may have implications for cancer immunotherapy.

### Discussion

In recent years, there has been a significant increase in the exploration of nanoparticles as a means of enhancing antitumor response and modulating the immune system. In particular, IONPs have been shown to be effective immunopotentiators in the treatment

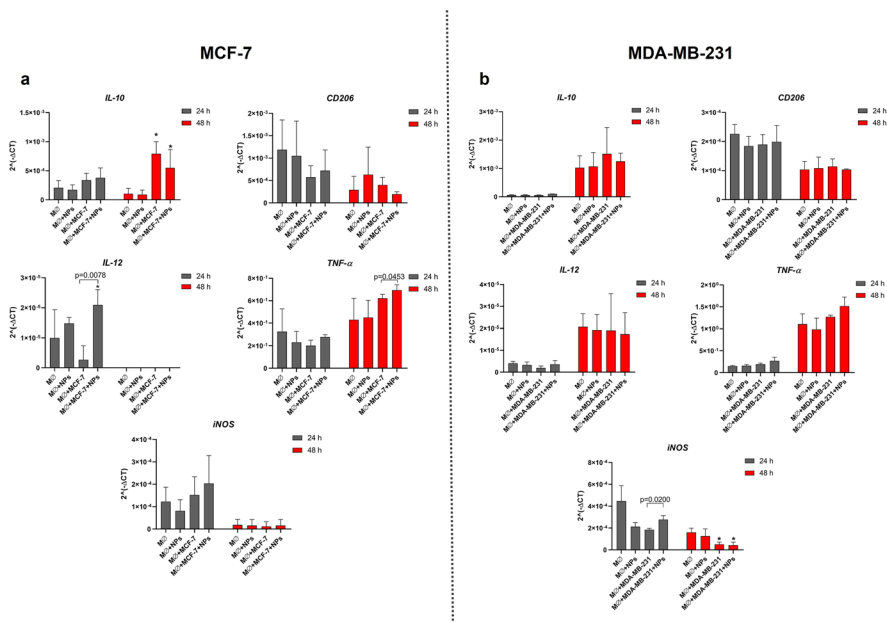


**Fig. 6** In **A** *IL-10*, *CD206*, *IL-12*, *TNF-α*, and *iNOS* expression in THP-1 macrophage co-cultured with MCF-7 cells. In **B** *IL-10*, *CD206*, *IL-12*, *TNF-α*, and *iNOS* expression in THP-1 macrophage co-cultured with MDA-MB-231 cells. Data are presented as mean ± standard deviation and are representative of five independent experiments. Statistical analysis was performed using paired t-test. (\*) p < 0.05 compared to macrophage control without stimulation. (Bar) p < 0.05 between co-cultures containing tumor cells and exposed and non-exposed macrophages to NPs, p-value indicated in the graph. NPs = Pani/γ-Fe<sub>2</sub>O<sub>3</sub>; MØ = macrophages

of various cancers, including breast cancer (Zanganeh et al. 2016; Costa da Silva et al. 1479; Zhang et al. 2020, 2019; Zhou et al. 2020; Jin et al. 2019; Gu et al. 2019; Dalzon et al. 2019; Mulens-Arias et al. 2021). In this study, we investigated the potential of Pani/γ-Fe<sub>2</sub>O<sub>3</sub> as a platform to modulate the polarization of macrophages in the tumor micro-environment and promote a tumor-suppressive pro-inflammatory phenotype.

For the use of IONPs in macrophage reprogramming assays, it is crucial to evaluate their biocompatibility before practical application. Therefore, we examined the viability of tumor cells and macrophages exposed to different concentrations of Pani/γ-Fe<sub>2</sub>O<sub>3</sub> NPs using the MTT assay. After 24 h of incubation, the Pani/γ-Fe<sub>2</sub>O<sub>3</sub> NPs showed obvious toxicity to THP-1 macrophages at concentrations above 0.06 mg/mL (60 μg/mL). As for the cytotoxicity of breast cancer cell lines, NPs generally showed toxicity at concentrations above 1.5 mg/mL (1500 μg/mL). The mechanisms by which Pani/γ-Fe<sub>2</sub>O<sub>3</sub> can be toxic to cells are already known. It has been shown that the cytotoxicity of colloidal dispersions of Pani/γ-Fe<sub>2</sub>O<sub>3</sub> NPs is directly related to the mass ratio between the Pani polymer, the γ-Fe<sub>2</sub>O<sub>3</sub> core, and the tested concentration in the culture medium (Bober et al. 2016). Furthermore, the Pani polymer itself induces cytotoxicity, as does its colloidal form (Humpolicek et al. 2012). It has also been demonstrated that the cytotoxicity of Pani is mainly due to the presence of ammonium persulfate (APS) and low molecular weight polar substances, as the APS is water-soluble, and its residues can be easily released from insoluble Pani when exposed to physiological conditions in the body (Kašpárková et al. 2019). Bober et al. (2016) evaluated the cytotoxicity of Pani/γ-Fe<sub>2</sub>O<sub>3</sub> NPs in mouse embryonic fibroblasts (NIH/3T3) and found that reducing the amount

of Pani in the colloid had a positive effect on cytocompatibility. However, reducing the amount of Pani below the critical limit should be avoided because the cytotoxicity results of this study also showed that the Pani/ $\gamma$ -Fe<sub>2</sub>O<sub>3</sub> colloid compound exhibited better cytocompatibility than pure  $\gamma$ -Fe<sub>2</sub>O<sub>3</sub>, paving the way for potential applications of such systems in biotechnology and biomedicine (Bober et al. 2016). As for the  $\gamma$ -Fe<sub>2</sub>O<sub>3</sub> core, the literature generally indicates that IONPs have low toxicity to mammalian models, which contributes to their use in biomedical applications (Petters et al. 2014). The results of this study indicate that Pani/ $\gamma$ -Fe<sub>2</sub>O<sub>3</sub> NPs have excellent cytocompatibility with the tested cells. In particular, at concentrations of  $\leq 0.06$  mg/mL (60  $\mu$ g/mL), these NPs showed good cytocompatibility with THP-1 macrophages, leading to their selection for transwell assay.

When assessing the effect of exposure to Pani/ $\gamma$ -Fe<sub>2</sub>O<sub>3</sub> NPs on co-cultures of macrophages and MCF-7 cells in a transwell system, a higher percentage of apoptotic MCF-7 cells was observed in cultures exposed to NPs, suggesting that the presence of NPs enhances the pro-apoptotic ability of macrophages. Previous in vitro and in vivo studies on the effect of IONPs in macrophage reprogramming confirmed that NPs are degraded in lysosomes after phagocytosis by macrophages, leading to intracellular iron accumulation (Weinstein et al. 2010). According to current knowledge, the intracellular oxidative stress caused by iron may be correlated with the activation of various iron-regulated genes (Gu et al. 2019). Accumulated iron may positively regulate ferritin levels in macrophages and reprogram these cells from an M2-like phenotype to an M1-like phenotype, increasing the expression of *CD86* and *TNF- $\alpha$*  genes (Laskar et al. 2013).

The results of the co-cultures between MCF -7 cells and THP-1 macrophages also showed that exposure to Pani/ $\gamma$ -Fe<sub>2</sub>O<sub>3</sub> NPs was able to reduce the levels of IL-1 $\beta$  in the culture supernatant and to increase the expression of genes related to the M1 profile (*IL-12* and *TNF- $\alpha$* ) in the macrophages. However, no changes were observed in the levels of oxidative stress markers. The increase in the percentage of apoptotic MCF-7 cells in the co-cultures exposed to Pani/ $\gamma$ -Fe<sub>2</sub>O<sub>3</sub> NPs may be related to the decrease in IL-1 $\beta$  secretion because TAMs have been described to protect colon cancer cells from apoptosis by secreting IL-1 $\beta$ . In the same study, it was found that inactivation of IL-1 $\beta$  by neutralization with an anti-IL-1 $\beta$  antibody or silencing of IL-1 $\beta$  inhibited the ability of macrophages to suppress apoptosis (Kaler et al. 2010). Studies have shown that IL-1 $\beta$  plays a divergent and contradictory role in the tumor microenvironment (Baker et al. 2019).

There is evidence to support the pro-tumorigenic role of IL-1 $\beta$ . For example, IL-1 $\beta$  is positively regulated in solid tumors such as breast cancer, colon cancer, lung cancer, head and neck cancer, and melanoma, and patients with IL-1 $\beta$  producing tumors generally have an unfavorable prognosis (Apte et al. 2006). Moreover, several in vitro and in vivo studies suggest that IL-1 $\beta$  plays a promoting role in tumor growth (Krelin et al. 2007). Another observation is that the production of IL-1 $\beta$  by myeloid cells in a melanoma model led to the activation of endothelial cells that produced VEGF and other pro-angiogenic factors, resulting in modulation of the tumor inflammatory microenvironment, increased angiogenesis, and tumor progression (Baston-Büst et al. 2012). However, other studies also highlight the ability of IL-1 $\beta$  to induce Th1 and Th17 responses, cells with potent anti-tumor properties (Baker et al. 2019). It has also been observed that IL-1 $\beta$  keeps metastatic cells in a differentiated state and prevents their establishment in

other parts of the body (Castaño et al. 2018). In contrast, another study provided evidence for the opposite role of IL-1 $\beta$ , leading to an increase in the invasive capacity of colon cancer cells (Li et al. 2012). Therefore, these conflicting results regarding IL-1 $\beta$  need to be carefully considered when developing cancer therapies aimed at inducing or inhibiting IL-1 $\beta$ .

Regarding macrophage gene expression in co-culture with MCF-7 cells, increased expression of *IL-12* and *TNF- $\alpha$*  genes showed that Pani/ $\gamma$ -Fe<sub>2</sub>O<sub>3</sub> NPs were able to increase gene expression associated with the M1 phenotype. Previous in vitro studies have shown that IONPs induce a phenotypic shift of macrophages toward an M1 profile with increased expression of *IL-12* and *TNF- $\alpha$*  (Zanganeh et al. 2016; Mulens-Arias et al. 2015). Moreover, this polarization toward an M1-like phenotype by IONPs may also trigger an increase in the Fenton reaction, a redox reaction in which Fe (II) is oxidized by H<sub>2</sub>O<sub>2</sub> to Fe (III), which in turn is reduced to the hydroxyl ion and hydroxyl radical, initiating programmed cell death of tumor cells by caspase 3/7-dependent apoptosis (Zanganeh et al. 2016). Despite the effects of ROS on cell apoptosis, the study showed that Pani/ $\gamma$ -Fe<sub>2</sub>O<sub>3</sub> NPs were unable to induce changes in the levels of oxidative stress markers in co-cultures of MCF-7 cells and macrophages. Therefore, the results suggest that the increased apoptosis of MCF-7 cells in such co-cultures may be related to the reduction of IL-1 $\beta$  secretion by macrophages.

It is important to note that of the various transcriptional reprogramming pathways that iron oxide nanoparticles can trigger in macrophages, some are related to various cell death processes such as apoptosis, ferroptosis, and autophagy. The balance between all signaling pathways activated by a particular IONP will determine the fate of the macrophage (Mulens-Arias et al. 2021).

In the co-cultures of MDA-MB-231 cells and macrophages exposed to Pani/ $\gamma$ -Fe<sub>2</sub>O<sub>3</sub> NPs, an increase in the percentage of dead cells (Sytox<sup>+</sup>/Caspase 3/7<sup>-</sup>) was observed. A significant increase in the levels of IL-6 and IL-1 $\beta$  was also observed in the cell-free medium of these co-cultures. The direct effect of IL-6 on breast cancer cell growth is not fully elucidated, and the results are contradictory: studies show direct growth inhibitory effects, while others show growth-promoting effects (Dethlefsen et al. 2013). Recent studies suggest that the inhibitory effect of IL-6 depends on the activation of the Jak/Stat3 pathway, which is active in more than 50% of breast cancer tumors and cell lines and plays a critical role in controlling growth, migration, and metastasis (Dethlefsen et al. 2013; Barbieri et al. 2010; Leslie et al. 2010). On the other hand, studies have shown that the response to IL-6 is also related to the status of hormone receptors, and no effect on proliferation, growth, or tumor inhibition was observed for the MDA-MB-231 cell line (Dethlefsen et al. 2013; Ásgeirsson et al. 1998; Johnston et al. 1992). Contrastingly, as mentioned earlier, the rise in production of the cytokine IL-1 $\beta$  is associated with safeguarding tumor cells against apoptosis. Nonetheless, IL-1 $\beta$  can also trigger cell death through a mechanism that necessitates the activation of p38MAPK and IKK $\beta$ , culminating in the upregulation of *iNOS* and the production of toxic levels of nitric oxide (Kaler et al. 2010; Vercaemmen et al. 2008). Aligned with this information, the co-culture assays further unveiled that exposure to Pani/ $\gamma$ -Fe<sub>2</sub>O<sub>3</sub> NPs resulted in increased *iNOS* gene expression in THP-1 macrophages and elevated levels of oxidative stress markers (malondialdehyde, carbonylated protein, and hydrogen peroxide), in the co-cultures,

indicating that the NPs induced oxidative stress in the THP-1 macrophage and MDA-MB-231 cell co-cultures. Importantly, it is recognized that an excess of ROS can lead to lipid peroxidation of cellular membranes, subsequently resulting in structural impairments that culminate in cell rupture and death through pathways distinct from apoptosis (Tang et al. 2019).

MDA-MB-231 represents a subtype of breast cancer known as triple-negative breast cancer (TNBC), constituting around 15–20% of all breast carcinomas. Perturbing statistics highlight that more than 50% of patients encounter a relapse within the initial 3–5 years following diagnosis, while the current therapeutic approaches yield a median overall survival of only 10.2 months (Li et al. 2022). Through our examination of this highly aggressive triple-negative breast cancer cell line, our investigation casts illumination on the efficacy of iron oxide nanoparticle-based therapy, furnishing valuable insights into its potential utility. The treatment of triple-negative breast cancer poses a substantial challenge due to its aggressive nature and the absence of actionable targets (Tarantino et al. 2022). Hence, the investigation of novel and innovative treatments for this subtype takes on extreme significance. Our research outcomes play a substantial role in the discovery of new treatments and have the potential to lay the basis for enhanced therapeutic strategies targeting triple-negative breast cancer.

The breast cancer cell lines MCF-7 and MDA-MB-231 display numerous phenotypic and genotypic disparities, and these variations could prove pivotal in elucidating the observed outcomes concerning the impact of iron oxide nanoparticles on macrophage reprogramming treatment (Theodossiou et al. 2019). It is important to emphasize that the selection of these two specific cell lines for this study was driven by the objective to comprehensively assess the therapeutic viability of  $\text{Pani}/\gamma\text{-Fe}_2\text{O}_3$  across a spectrum that encompasses highly diverse forms of breast cancer. Our research outcomes elucidate that variations in receptor status among these cell lines yield diverse treatment responses and distinctive cellular behaviors. Considering the observed dissonance in cytokine profiles between the two cell lines, we can infer that these profiles significantly underpin discrepant outcomes in both macrophage reprogramming and treatment responsiveness. Cytokines play a central role as primary mediators within the complex mechanisms of tumor development and metastasis. Certain cytokines not only enhance the tumor's skill in evading immune surveillance but also manipulate immune system responses to its benefit (Chen et al. 2020). Moreover, cytokine levels have been correlated with tumor stage, survival, and malignancy, making them potential prognostic factors, in addition to their impact on tumor progression (Esquivel-Velázquez et al. 2015). Furthermore, there exists a correlation between cytokine levels and crucial tumor aspects such as stage, survival rates, and malignancy. This correlation positions cytokines as potential prognostic factors, supplementing their influence on the progression of tumors (Theodossiou et al. 2019).

It is important to note that the development of studies based on macrophage reprogramming using IONPs remains largely empirical. The lack of standardization of pre-clinical studies and the variability of experimental conditions and results still represents a barrier to the creation of IONP-based therapies (Nascimento et al. 2021). Breast cancer is a highly heterogeneous disease, and recent genome analyses have shown that breast cancer cells accumulate more than 1,000 mutations (Koboldt et al. 2012). This

genetic diversity is reflected by the multiplicity of breast cancer types, each with a different prognosis and approach to treatment (Dethlefsen et al. 2013). In our *in vitro* study, the results indicated that exposure to Pani/ $\gamma$ -Fe<sub>2</sub>O<sub>3</sub> NPs was capable of enhancing macrophage-induced cell death in tumor cell lines through various pathways. Additionally, these nanoparticles demonstrated the ability to modulate biomolecules that are pertinent to susceptibility or resistance in breast cancer.

Hence, it is important to conduct additional research on the utilization of iron oxide nanoparticles to reprogram macrophages for breast cancer treatment. This endeavor is crucial for advancing our comprehension of the underlying mechanisms and maximizing therapeutic efficacy. Moreover, a comprehensive exploration of potential side effects and nanoparticle toxicity is essential to ensure their secure implementation in clinical contexts. Ultimately, the outcomes of such research could pave the way for the creation of enhanced, personalized approaches for treating breast cancer patients.

## Conclusion

The findings from this study offer compelling evidence that the Pani/ $\gamma$ -Fe<sub>2</sub>O<sub>3</sub> nanoparticles exhibit favorable attributes for utilization in biological systems, including their cytocompatibility. Particularly noteworthy are the outcomes of *in vitro* co-culture experiments, which reveal the nanoparticles' potential to redirect macrophages toward an M1 phenotype characterized by tumor-suppressive traits. The alterations observed in gene expression upon exposure to these nanoparticles bring about changes in the profiles of pro-inflammatory cytokines and the production of reactive oxygen species (ROS) in the culture supernatants. These modifications ultimately culminate in the demise of specific types of tumor cells through distinct pathways.

The results of this study have important implications for the advancement of innovative strategies in cancer treatment that focus on the tumor microenvironment. Specifically, the ability of Pani/ $\gamma$ -Fe<sub>2</sub>O<sub>3</sub> nanoparticles to shift macrophage behavior toward an anti-tumor state, alongside their capacity to induce oxidative stress and trigger cancer cell death, positions them as promising candidates for further exploration in animal models. However, it's important to recognize that the lack of consistent approaches in preclinical studies, along with the inherent diversity of breast cancer, presents significant challenges when developing effective nanoparticle-based therapies.

Future research should prioritize addressing these challenges and uncovering the mechanisms behind the observed effects of Pani/ $\gamma$ -Fe<sub>2</sub>O<sub>3</sub> nanoparticles on macrophages and tumor cells. Such studies could lay the groundwork for innovative nanotherapeutic strategies that manipulate the tumor microenvironment and enhance the effectiveness of existing cancer treatments.

## Methods

### Synthesis and physicochemical characterization of maghemite nanoparticles coated with polyaniline

Nanoparticles were developed at the Laboratory of Unconventional Polymers—LPNC, at the Department of Physics of the Federal University of Pernambuco. Maghemite nanoparticles coated with polyaniline were synthesized using the co-precipitation method (Medina-Llamas et al. 2014). Specific production and characterization data

can be viewed in our group's previous study (Nascimento et al. 2023). In general, the nanoparticles have a cuboid/spherical morphology and an average diameter of  $37.87 \pm 6.48$  nm. TEM micrograph of Pani/ $\gamma$ -Fe<sub>2</sub>O<sub>3</sub> NPs is presented in Additional file 1: Figure S1. Nanoparticles have a hydrodynamic size of  $442.78 \pm 145.99$  nm, which corresponds to the size of the nanoparticle cluster, a polydispersity index of  $0.4 \pm 0.08$ , and a zeta potential of  $-24.81 \pm 0.38$  mV.

### Cells and culturing

MCF-7, MDA-MB-231, and THP-1 cells were obtained from the Banco de Células do Rio de Janeiro (BCRJ). Human breast cancer cells (MCF-7 and MDA-MB-231) were cultured in Dulbecco's Modified Eagle's Medium (DMEM) (Gibco) supplemented with 10% heat-inactivated fetal bovine serum (FBS) (Gibco), 1% penicillin (100 IU/mL), and streptomycin (100 mg/mL) (PenStrep) (Gibco) and incubated at 37 °C in a humidified atmosphere containing 5% CO<sub>2</sub>. THP-1 cells were cultured in RPMI-1640 (ATCC modification) (Gibco) supplemented with 10% FBS (Gibco), 1% PenStrep (100 IU/mL) (Gibco), and incubated at 37 °C in a humidified atmosphere containing 5% CO<sub>2</sub>.

### Differentiation of THP-1 monocytes into macrophages

To differentiate the THP-1 monocyte lineage into macrophages, cells were treated with 320 nM of phorbol 12-myristate 13-acetate (PMA) (Sigma-Aldrich) for 24 h. After this time, the culture medium was removed, and the cells were washed with 1X phosphate-buffered Saline (PBS), pH 7.2, and incubated for an additional 24 h in DMEM culture medium supplemented with 10% FBS and 1% PenStrep. The cells were maintained in a 5% CO<sub>2</sub> and 37 °C incubator throughout the differentiation process.

### Nanoparticles biocompatibility

To obtain a non-cytotoxic concentration suitable for co-culture assays using a transwell system, we evaluated the cytotoxicity of Pani/ $\gamma$ -Fe<sub>2</sub>O<sub>3</sub> nanoparticles (NPs) on breast cancer cell lines (MCF-7, MDA-MB-231) and THP-1 cells differentiated into macrophages.

For the tumor cell lines, we seeded cells in 24-well plates at a density of  $2 \times 10^5$  cells per well and cultured them in DMEM medium supplemented with 10% FBS and 1% PenStrep for 24 h. For THP-1 cells, cells were seeded in 12-well plates at a density of  $3.8 \times 10^5$  cells per well and differentiated into macrophages by culturing them in DMEM medium supplemented with 10% FBS, 1% PenStrep, and 320 nM PMA for 24 h. All cells were incubated in a CO<sub>2</sub> incubator at 37 °C.

After the incubation period, cells were exposed to Pani/ $\gamma$ -Fe<sub>2</sub>O<sub>3</sub> NPs at concentrations of 0.5, 1, 1.5, 3, 6, and 9 mg/mL for 24 h (Zanganeh et al. 2016). For THP-1 cells exposure to Pani/ $\gamma$ -Fe<sub>2</sub>O<sub>3</sub> concentrations of 0.01, 0.03, 0.06, 0.12, and 0.25 mg/mL was also evaluated since the range 0.5–9 mg/mL was cytotoxicity. After exposure, the MTT ([3-(4,5-dimethylthiazol-2-yl)-2,5-diphenyltetrazolium] bromide) (Invitrogen) method was performed to evaluate cell viability. Briefly, an MTT solution at a concentration of 0.5 mg/mL was prepared by dissolving the salt in DMEM medium supplemented with 10% FBS and 1% PenStrep. The culture medium in the wells was removed, and the cells were washed three times with PBS 1X (pH 7.2). Next, 1 mL of the MTT solution was added to each well, and the plates were incubated at 37 °C for 2 h. After incubation, the

MTT solution was removed from the wells, and 1 mL of dimethyl sulfoxide (DMSO) (Sigma-Aldrich) was added to each well. The plates were then placed on a plate shaker (ICell) for 5 min to dissolve the formazan crystals, followed by a 5-min resting period for color stabilization. The resulting, purple-colored solution was transferred to a 96-well plate (Sarstedt), and the optical density (OD) was measured using a Spectramax 340pc plate reader (Molecular Devices) at a wavelength of 570 nm. Cell viability was calculated using the following formula: (mean absorbance of treated samples/mean absorbance of control samples)  $\times$  100. After analyzing the data, the maximum non-cytotoxic concentration of the nanoparticles was selected for each cell line, and this concentration was used for the co-culture *in vitro* assays.

### Transwell assays

Differentiated THP-1 monocytes into macrophages ( $1.8 \times 10^5$  cells per well) and MCF-7 and MDA-MB-231 tumor cells ( $3.6 \times 10^5$  cells per well) were co-cultured using a transwell system (Sigma-Aldrich), with a 0.4  $\mu$ m membrane in DMEM culture medium containing 10% FBS and 1% PenStrep. Macrophages were positioned in the upper chamber and tumor cells in the lower chamber. Transwell inserts provide a cell co-culture environment that closely emulates *in vivo* conditions. The presence of 0.4  $\mu$ m pores in the insert membrane facilitates a dynamic interaction between the two cell types. Moreover, utilizing this system enhances our comprehension of Pani's influence on macrophage reprogramming within the co-culture context involving breast cancer tumor cells, thereby yielding invaluable insights for our study. The decision to maintain a tumor cell-to-macrophage ratio of 2:1 stems from the recognition that, in the context of breast cancer, M2 TAMs can constitute up to 50% of the tumor's cellular mass (Solinas et al. 2009).

After 24 and 48 h of exposure, tumor cells were labeled with CellEvent™ Caspase-3/7 Green Flow Cytometry Assay (Invitrogen) and SYTOX® AADvanced dead cell stain (Invitrogen), according to the manufacturer's instructions. Briefly, 1  $\mu$ L of the CellEvent™ Caspase-3/7 Green Detection Reagent (500 nM) was added to each well of the plate containing tumor cells. The samples were incubated for 30 min at 37 °C, protected from light. During the last 5 min of staining, 1  $\mu$ L of SYTOX™ AADvanced™ solution (1  $\mu$ M) was added to each well of the plate containing tumor cells, and the samples were incubated at 37 °C. After the labeling procedure, the cells were collected in 15 mL tubes. Next, centrifugation was performed at 1000 rpm for 10 min, and the samples were suspended in 300  $\mu$ L of PBS 1X followed by transfer to 5 mL polystyrene tubes (BD Biosciences). The samples were analyzed using excitation of 488 nm and collecting fluorescence emission using a 530/30 bandpass filter and a 690/50 bandpass filter. A total of 100,000 events were acquired in the LSR Fortessa flow cytometer (BD Biosciences). Compensation was performed with polystyrene microparticles conjugated with anti-mouse Kappa chain antibodies (BD Compbeads anti-mouse, BD Biosciences).

### Cytokine profile

To determine the cytokine profile in the co-culture system, the CBA Human Inflammatory Cytokines Kit (BD Biosciences) was used to measure the cytokines IL-1 $\beta$ , IL-6, IL-8, IL-10, TNF- $\alpha$ , and IL-12p70 in the medium. The protocol was performed according to the manufacturer's instructions. A total of 2100 events (350 per bead) were acquired



on the FACS Verse flow cytometer (BD Biosciences) and the data were analyzed using FCAP Array™ V3.0 software (BD Biosciences).

### Gene expression analysis

Total RNA was extracted from macrophages obtained from the co-culture with tumor cells using the PureLink™ RNA Mini Kit (ThermoFisher Scientific). The purified RNA was transcribed into cDNA using the High-Capacity RNA-to-cDNA kit (Applied Biosystems) following the manufacturer's instructions. *GAPDH* was used as the constitutive expression gene.

The mRNA of the constitutive expression gene and the genes of interest were amplified and detected using the TaqMan® probe system (Applied Biosystems): *GAPDH* (Hs02758991\_m1), *CD80* (Hs01045161\_m1), *CD86* (Hs1567026\_m1), *ARG1* (Hs500163660\_m1), *IL-12B* (Hs01011518\_m1), *iNOS* (Hs01075529), *MRC1* (Hs00961622), *IL-10* (Hs00961622) and *TNF-α* (Hs00174128) according to the manufacturer's instructions. The cycling was performed using the ViiA 7 Real-Time PCR System (Applied Biosystems). Reactions were executed in triplicate in a 10 µL volume, with the following cycle parameters: enzyme activation (10 min at 95 °C), followed by 40 cycles (each cycle consisting of 15 s at 95 °C and 1 min at 60 °C). The cycle threshold was automatically determined by the QuantStudio™ 6 and 7 Flex Real-Time PCR System Software (Applied Biosystems). Data analysis was performed using the  $2^{-\Delta C_t}$  method (Schmittgen and Livak 2008). Samples with no expression of the gene of interest were considered  $2^{-\Delta C_t} = 0$ .

### Oxidative stress markers assays

The detection of malondialdehyde (MDA) content in culture supernatants is a useful indicator of lipid peroxidation in cells, and therefore, the level of cellular damage caused by oxidative stress. MDA is a catabolic product of lipid peroxidation that reacts with thiobarbituric acid (TBA) to produce a red compound with a maximum absorption peak at 532 nm. To quantify MDA levels, it was used the malondialdehyde colorimetric assay kit (Elabscience Biotechnology) followed the manufacturer's protocol. The OD was measured using a Spectramax 340pc plate reader (Molecular Devices) at a wavelength of 532 nm.

To measure hydrogen peroxide levels, we used the Pierce™ Quantitative Peroxide Assay (aqueous-compatible formulation) commercial kit (Thermo Scientific). This assay uses an iron and xylenol orange reagent to detect and measure hydrogen peroxide levels in biological samples. The OD was measured using a Spectramax 340pc plate reader (Molecular Devices) at a wavelength of 595 nm.

Protein oxidation by ROS can lead to the production of carbonyl groups, which are an indicator of oxidative damage. We measured the carbonyl group content using the Protein Carbonyl Content Assay commercial kit (Sigma-Aldrich) according to the manufacturer's protocol. This assay involves the derivatization of protein carbonyl groups by 2,4-dinitrophenylhydrazine (DNPH), which forms stable dinitrophenylhydrazone (DNP) adducts. The OD was measured using a Spectramax 340pc plate reader (Molecular Devices) at a wavelength of 375 nm.

For the calculations of MDA and carbonyl group content, it was determined the protein content using the Pierce™ BCA Protein Assay kit (Thermo Scientific), following the manufacturer's protocol.

### Statistical analysis

All statistical analyses were performed using GraphPad Prism version 6.04 (GraphPad Software). Results are expressed as mean ± standard deviation (s.d.) of at least three independent experiments. Data normality was previously evaluated using the Shapiro–Wilk test. Kruskal–Wallis test followed by Dunn's test for non-normally distributed groups. Paired group comparisons were conducted using the paired t-test for normally distributed groups. Values of  $p < 0.05$  were considered statistically significant.

### Abbreviations

ARG1	Arginase 1
CBA	Cytometric bead array
DMEM	Dulbecco's Modified Eagle Medium
DMSO	Dimethyl sulfoxide
DMT-1	Divalent metal transporter-1
FBS	Fetal bovine serum
GAPDH	Glyceraldehyde 3-phosphate dehydrogenase
HO-1	Heme oxygenase
iNOS	Inducible nitric oxide synthase
IONPs	Iron oxide nanoparticles
MDA	Malondialdehyde
MRC1	Mannose receptor C-type 1
MTT	3-(4,5-Dimethylthiazol-2-yl)-2,5-diphenyltetrazolium Bromide
NPs	Nanoparticles
OD	Optical density
PBS	Phosphate-buffered saline
PCR	Polymerase chain reaction
PenStrep	Penicillin, streptomycin, and amphotericin B
PMA	Phorbol 12-myristate 13-acetate
RNS	Reactive nitrogen species
ROS	Reactive oxygen species
RPMI 1640	Roswell Park Memorial Institute 1640
RT-qPCR	Real-time quantitative reverse transcription PCR
TAMs	Tumor-associated macrophages
TBA	Thiobarbituric acid

### Supplementary Information

The online version contains supplementary material available at <https://doi.org/10.1186/s12645-023-00225-3>.

**Additional file 1: Fig. S1** Transmission electron microscopy micrographs of Pani/ $\gamma$ -Fe<sub>2</sub>O<sub>3</sub> nanoparticles clusters. The white bar indicates the scale. **Fig. S2** Uptake of NPs of Pani/ $\gamma$ -Fe<sub>2</sub>O<sub>3</sub> by THP-1 macrophages. a) Brightfield microscopy images of Pani/ $\gamma$ -Fe<sub>2</sub>O<sub>3</sub> nanoparticles obtained by ZOE Fluorescent Cell Imager (Scinomics). b) Transmission electron microscopy micrograph of Pani/ $\gamma$ -Fe<sub>2</sub>O<sub>3</sub> nanoparticles into macrophages. Pani/ $\gamma$ -Fe<sub>2</sub>O<sub>3</sub> nanoparticles were mainly observed in endosome structures of macrophages (black dots and red arrows). The nanoparticle aggregates (black

dots) appeared randomly distributed throughout the cytoplasm of macrophages. The black and white bars indicate the scale.

### Acknowledgements

The authors thank the René Rachou Institute /FIOCRUZ Minas, Real-Time PCR, and flow cytometry platforms. They also thank the Programa de Pós-graduação em Ciências da Saúde of the René Rachou Institute /FIOCRUZ Minas and the Coordenadoria de Aperfeiçoamento de Pessoal de Nível Superior (CAPES).

### Author contributions

CN conducted the investigation, performed experiments, analyzed and interpreted data, and drafted the manuscript. NT, IB, MC, EO, SC, and AL contributed to experimental work and manuscript revisions. RC-O, EA, and CM reviewed the data and provided critical revisions to the manuscript. CC-S conceptualized the study, supervised the research, and contributed to writing the paper.

### Funding

This study was financially supported by Coordenadoria de Aperfeiçoamento de Pessoal de Nível Superior (CAPES)—Finance Code 001 and FAPEMIG—Rede Mineira de Nanomedicina Teranóstica (RED-00079-22).

### Availability of data and materials

All data generated or analyzed during this study are included in this published article.

### Declarations

#### Ethics approval and consent to participate

Not applicable.

#### Consent for publication

Not applicable.

#### Competing interests

The authors declare that they have no competing interests.

Received: 3 July 2023 Accepted: 28 August 2023

Published online: 07 September 2023

### References

- Apte RN, Krelin Y, Song X, Dotan S, Rech E, Elkabets M et al (2006) Effects of micro-environment- and malignant cell-derived interleukin-1 in carcinogenesis, tumour invasiveness and tumour–host interactions. *Eur J Cancer* 42:751–759. <https://doi.org/10.1016/j.ejca.2006.01.010>
- Arnold M, Morgan E, Rungay H, Mafra A, Singh D, Laversanne M et al (2022) The current and future burden of breast cancer: global statistics for 2020 and 2040. *The Breast* 66:15–23. <https://doi.org/10.1016/j.breast.2022.08.010>
- Ásgeirsson KS, Ólafsdóttir K, Jónasson JG, Ögmundsdóttir HM (1998) The effects of il-6 on cell adhesion and e-cadherin expression in breast cancer. *Cytokine* 10:720–728. <https://doi.org/10.1006/cyto.1998.0349>
- Baker KJ, Houston A, Brint E (2019) IL-1 family members in cancer; two sides to every story. *Front Immunol* 10:1197. <https://doi.org/10.3389/fimmu.2019.01197>
- Barbieri I, Pensa S, Pannellini T, Quagliano E, Maritano D, Demaria M et al (2010) Constitutively active Stat3 enhances neu-mediated migration and metastasis in mammary tumors via upregulation of cten. *Cancer Res* 70:2558–2567. <https://doi.org/10.1158/0008-5472.CAN-09-2840>
- Baston-Büst D, Böddeker SJ, Altergot O, Ziegler D, Krüssel J-S, Hess AP (2012) Angiogenic factor composition of decidualized endometrial stromal cells is modified by knock-down of syndecan-1 followed by imitation of embryo contact. *J Reprod Immunol* 94:59–60. <https://doi.org/10.1016/j.jri.2012.03.347>
- Biswas SK, Mantovani A (2010) Macrophage plasticity and interaction with lymphocyte subsets: cancer as a paradigm. *Nat Immunol* 11:889–896. <https://doi.org/10.1038/ni.1937>
- Biswas SK, Mantovani A (2012) Orchestration of metabolism by macrophages. *Cell Metab* 15:432–437. <https://doi.org/10.1016/j.cmet.2011.11.013>
- Bober P, Zasonska BA, Humpolíček P, Kuceková Z, Varga M, Horák D et al (2016) Polyaniline–maghemite based dispersion: electrical, magnetic properties and their cytotoxicity. *Synth Met* 214:23–29. <https://doi.org/10.1016/j.synthmet.2016.01.010>
- Castaño Z, San Juan BP, Spiegel A, Pant A, DeCristo MJ, Laszewski T et al (2018) IL-1 $\beta$  inflammatory response driven by primary breast cancer prevents metastasis-initiating cell colonization. *Nat Cell Biol*. <https://doi.org/10.1038/s41556-018-0173-5>
- Chen K, Satlof L, Stoffels G, Kothapalli U, Ziluck N, Lema M et al (2020) Cytokine secretion in breast cancer cells—MILLI-PLEX assay data. *Data Brief* 28:104798. <https://doi.org/10.1016/j.dib.2019.104798>
- Colleoni M, Sun Z, Price KN, Karlsson P, Forbes JF, Thürlimann B et al (2016) Annual hazard rates of recurrence for breast cancer during 24 years of follow-up: results from the international breast cancer study group trials I to V. *J Clin Oncol* 34:927–935. <https://doi.org/10.1200/JCO.2015.62.3504>

- Corna G, Campana L, Pignatti E, Castiglioni A, Tagliafico E, Bosurgi L et al (2010) Polarization dictates iron handling by inflammatory and alternatively activated macrophages. *Haematologica* 95:1814–1822. <https://doi.org/10.3324/haematol.2010.023879>
- Costada Silva M, Breckwoldt MO, Vinchi F, Correia MP, Stojanovic A, Thielmann CM et al (2017) Iron induces anti-tumor activity in tumor-associated macrophages. *Front Immunol* 8:1479. <https://doi.org/10.3389/fimmu.2017.01479>
- Cronin SJF, Woolf CJ, Weiss G, Penninger JM (2019) The role of iron regulation in immunometabolism and immune-related disease. *Front Mol Biosci* 6:116. <https://doi.org/10.3389/fmolb.2019.00116>
- Dalzon B, Guidetti M, Testemale D, Reymond S, Proux O, Voltaire J et al (2019) Utility of macrophages in an antitumor strategy based on the vectorization of iron oxide nanoparticles. *Nanoscale* 11:9341–9352. <https://doi.org/10.1039/C8NR03364A>
- Dethlefsen C, Højfeldt G, Hojman P (2013) The role of intratumoral and systemic IL-6 in breast cancer. *Breast Cancer Res Treat* 138:657–664. <https://doi.org/10.1007/s10549-013-2488-z>
- Esquivel-Velázquez M, Ostoa-Saloma P, Palacios-Arreola MI, Nava-Castro KE, Castro JI, Morales-Montor J (2015) The role of cytokines in breast cancer development and progression. *J Interferon Cytokine Res* 35:1–16. <https://doi.org/10.1089/jir.2014.0026>
- Gu Z, Liu T, Tang J, Yang Y, Song H, Tuong ZK et al (2019) Mechanism of iron oxide-induced macrophage activation: the impact of composition and the underlying signaling pathway. *J Am Chem Soc* 141:6122–6126. <https://doi.org/10.1021/jacs.8b10904>
- Harbeck N, Gnant M (2017) Breast cancer. *The Lancet* 389:1134–1150. [https://doi.org/10.1016/S0140-6736\(16\)31891-8](https://doi.org/10.1016/S0140-6736(16)31891-8)
- Huang A, Cao S, Tang L (2017) The tumor microenvironment and inflammatory breast cancer. *J Cancer* 8:1884–1891. <https://doi.org/10.7150/jca.17595>
- Humpolicek P, Kasparkova V, Saha P, Stejskal J (2012) Biocompatibility of polyaniline. *Synth Met* 162:722–727. <https://doi.org/10.1016/j.synthmet.2012.02.024>
- Jin R, Liu L, Zhu W, Li D, Yang L, Duan J et al (2019) Iron oxide nanoparticles promote macrophage autophagy and inflammatory response through activation of toll-like Receptor-4 signaling. *Biomaterials* 203:23–30. <https://doi.org/10.1016/j.biomaterials.2019.02.026>
- Johnston PG, Rondinone CM, Voeller D, Allegra CJ (1992) Identification of a protein factor secreted by 3T3-L1 preadipocytes inhibitory for the human MCF-7 breast cancer cell line. *Cancer Res* 52:6860–6865
- Jung M, Mertens C, Tomat E, Brüne B (2019) Iron as a central player and promising target in cancer progression. *Int J Mol Sci* 20:273. <https://doi.org/10.3390/ijms20020273>
- Kaler P, Galea V, Augenlicht L, Klampfer L (2010) Tumor associated macrophages protect colon cancer cells from TRAIL-induced apoptosis through IL-1 $\beta$ -dependent stabilization of snail in tumor cells. *PLoS ONE* 5:e11700. <https://doi.org/10.1371/journal.pone.0011700>
- Kašpárková V, Humpolicek P, Stejskal J, Capáková Z, Bober P, Skopalová K et al (2019) Exploring the critical factors limiting polyaniline biocompatibility. *Polymers (basel)* 11:362. <https://doi.org/10.3390/polym11020362>
- Kerr AJ, Dodwell D, McGale P, Holt F, Duane F, Mannu G et al (2022) Adjuvant and neoadjuvant breast cancer treatments: a systematic review of their effects on mortality. *Cancer Treat Rev* 105:102375. <https://doi.org/10.1016/j.ctr.2022.102375>
- Koboldt DC, Fulton RS, McLellan MD, Schmidt H, Kalicki-Verizer J, McMichael JF et al (2012) Comprehensive molecular portraits of human breast tumours. *Nature* 490:61–70. <https://doi.org/10.1038/nature11412>
- Krelin Y, Voronov E, Dotan S, Elkabets M, Reich E, Fogel M et al (2007) Interleukin-1 $\beta$ -driven inflammation promotes the development and invasiveness of chemical carcinogen-induced tumors. *Cancer Res* 67:1062–1071. <https://doi.org/10.1158/0008-5472.CAN-06-2956>
- Laskar A, Eilertsen J, Li W, Yuan X-M (2013) SPION primes THP1 derived M2 macrophages towards M1-like macrophages. *Biochem Biophys Res Commun* 441:737–742. <https://doi.org/10.1016/j.bbrc.2013.10.115>
- Leslie K, Gao SP, Berishaj M, Podsypanina K, Ho H, Ivashkiv L et al (2010) Differential interleukin-6/Stat3 signaling as a function of cellular context mediates Ras-induced transformation. *Breast Cancer Res* 12:R80. <https://doi.org/10.1186/bcr2725>
- Li Y, Wang L, Pappan L, Galliher-Beckley A, Shi J (2012) IL-1 $\beta$  promotes stemness and invasiveness of colon cancer cells through Zeb1 activation. *Mol Cancer*. <https://doi.org/10.1186/1476-4598-11-87>
- Li Y, Zhang H, Merker Y, Chen L, Liu N, Leonov S et al (2022) Recent advances in therapeutic strategies for triple-negative breast cancer. *J Hematol Oncol* 15:121. <https://doi.org/10.1186/s13045-022-01341-0>
- Mantovani A, Sica A, Sozzani S, Allavena P, Vecchi A, Locati M (2004) The chemokine system is in diverse forms of macrophage activation and polarization. *Trends Immunol* 25:677–686. <https://doi.org/10.1016/j.it.2004.09.015>
- Mantovani A, Marchesi F, Malesci A, Laghi L, Allavena P (2017) Tumour-associated macrophages as treatment targets in oncology. *Nat Rev Clin Oncol* 14:399–416. <https://doi.org/10.1038/nrclinonc.2016.217>
- Medina-Llamas JC, Chávez-Guajardo AE, Andrade CAS, Alves KGB, de Melo CP (2014) Use of magnetic polyaniline/magnetite nanocomposite for DNA retrieval from aqueous solutions. *J Colloid Interface Sci* 434:167–174. <https://doi.org/10.1016/j.jcis.2014.08.002>
- Mulens-Arias V, Rojas JM, Pérez-Yagüe S, Morales MP, Barber DF (2015) Polyethylenimine-coated SPIONs trigger macrophage activation through TLR-4 signaling and ROS production and modulate podosome dynamics. *Biomaterials* 52:494–506. <https://doi.org/10.1016/j.biomaterials.2015.02.068>
- Mulens-Arias V, Rojas JM, Barber DF (2021) The use of iron oxide nanoparticles to reprogram macrophage responses and the immunological tumor microenvironment. *Front Immunol* 12:693709. <https://doi.org/10.3389/fimmu.2021.693709>
- Murray PJ, Allen JE, Biswas SK, Fisher EA, Gilroy DW, Goerdt S et al (2014) Macrophage activation and polarization: nomenclature and experimental guidelines. *Immunity* 41:14–20. <https://doi.org/10.1016/j.immuni.2014.06.008>
- Nascimento CS, Alves ÉAR, de Melo CP, Corrêa-Oliveira R, Calzavara-Silva CE (2021) Immunotherapy for cancer: effects of iron oxide nanoparticles on polarization of tumor-associated macrophages. *Nanomedicine* 16:2633–2650. <https://doi.org/10.2217/nmm-2021-0255>

- Nascimento C, Castro F, Domingues M, Lage A, Alves É, de Oliveira R et al (2023) Reprogramming of tumor-associated macrophages by polyaniline-coated iron oxide nanoparticles applied to treatment of breast cancer. *Int J Pharm* 636:122866. <https://doi.org/10.1016/j.ijpharm.2023.122866>
- Petters C, Irrsack E, Koch M, Dringen R (2014) Uptake and metabolism of iron oxide nanoparticles in brain cells. *Neurochem Res* 39:1648–1660. <https://doi.org/10.1007/s11064-014-1380-5>
- Recalcati S, Cairo G (2021) Macrophages and iron: a special relationship. *Biomedicines*. <https://doi.org/10.3390/biomedicines9111585>
- Schmittgen TD, Livak KJ (2008) Analyzing real-time PCR data by the comparative CT method. *Nat Protoc* 3:1101–1108. <https://doi.org/10.1038/nprot.2008.73>
- Solinas G, Germano G, Mantovani A, Allavena P (2009) Tumor-associated macrophages (TAM) as major players of the cancer-related inflammation. *J Leukoc Biol* 86:1065–1073. <https://doi.org/10.1189/jlb.0609385>
- Sung H, Ferlay J, Siegel RL, Laversanne M, Soerjomataram I, Jemal A et al (2021) Global Cancer Statistics 2020: GLOBOCAN Estimates of Incidence and Mortality Worldwide for 36 Cancers in 185 Countries. *CA Cancer J Clin* 71:209–249. <https://doi.org/10.3322/caac.21660>
- Tang D, Kang R, Berghe TV, Vandenabeele P, Kroemer G (2019) The molecular machinery of regulated cell death. *Cell Res* 29:347–364. <https://doi.org/10.1038/s41422-019-0164-5>
- Tarantino P, Corti C, Schmid P, Cortes J, Mittendorf EA, Rugo H et al (2022) Immunotherapy for early triple negative breast cancer: research agenda for the next decade. *NPJ Breast Cancer* 8:23. <https://doi.org/10.1038/s41523-022-00386-1>
- Theodosiou TA, Ali M, Grigalavicius M, Gallart B, Dillard P, Schink KO et al (2019) Simultaneous defeat of MCF7 and MDA-MB-231 resistances by a hypericin PDT–tamoxifen hybrid therapy. *NPJ Breast Cancer* 5:13. <https://doi.org/10.1038/s41523-019-0108-8>
- Vercammen E, Staal J, Van Den Broeke A, Haegman M, Vereecke L, Schotte P et al (2008) Prolonged exposure to IL-1 $\beta$  and IFN $\gamma$  induces necrosis of L929 tumor cells via a p38MAPK/NF- $\kappa$ B/NO-dependent mechanism. *Oncogene* 27:3780–3788. <https://doi.org/10.1038/onc.2008.4>
- Weagel E, Curren S, Liu PG, Robison R, O'Neill K (2015) Macrophage polarization and its role in cancer. *J Clin Cell Immunol* 6:338. <https://doi.org/10.4172/2155-9899.1000338>
- Weinstein JS, Varallyay CG, Dosa E, Gahramanov S, Hamilton B, Rooney WD et al (2010) Superparamagnetic iron oxide nanoparticles: diagnostic magnetic resonance imaging and potential therapeutic applications in neurooncology and central nervous system inflammatory pathologies, a review. *J Cereb Blood Flow Metab* 30:15–35. <https://doi.org/10.1038/jcbfm.2009.192>
- Zanganeh S, Hutter G, Spittler R, Lenkov O, Mahmoudi M, Shaw A et al (2016) Iron oxide nanoparticles inhibit tumour growth by inducing pro-inflammatory macrophage polarization in tumour tissues. *Nat Nanotechnol* 11:986–994. <https://doi.org/10.1038/nnano.2016.168>
- Zhang L, Tan S, Liu Y, Xie H, Luo B, Wang J (2019) In vitro inhibition of tumor growth by low-dose iron oxide nanoparticles activating macrophages. *J Biomater Appl* 33:935–945. <https://doi.org/10.1177/0885328218817939>
- Zhang W, Cao S, Liang S, Tan CH, Luo B, Xu X et al (2020) Differently charged super-paramagnetic iron oxide nanoparticles preferentially induced M1-like phenotype of macrophages. *Front Bioeng Biotechnol* 8:537. <https://doi.org/10.3389/fbioe.2020.00537>
- Zhou Y, Que K-T, Tang H-M, Zhang P, Fu Q-M, Liu Z-J (2020) Anti-CD206 antibody-conjugated Fe<sub>3</sub>O<sub>4</sub>-based PLGA nanoparticles selectively promote tumor-associated macrophages to polarize to the pro-inflammatory subtype. *Oncol Lett* 20:1–10. <https://doi.org/10.3892/ol.2020.12161>

## Publisher's Note

Springer Nature remains neutral with regard to jurisdictional claims in published maps and institutional affiliations.

Ready to submit your research? Choose BMC and benefit from:

- fast, convenient online submission
- thorough peer review by experienced researchers in your field
- rapid publication on acceptance
- support for research data, including large and complex data types
- gold Open Access which fosters wider collaboration and increased citations
- maximum visibility for your research: over 100M website views per year

At BMC, research is always in progress.

Learn more [biomedcentral.com/submissions](https://biomedcentral.com/submissions)

